Contents lists available at GrowingScience

Current Chemistry Letters

homepage: www.GrowingScience.com

Antifungal potential of mannopyranoside derivatives through computational and molecular docking studies against *Candida albicans* 1IYL and 1AI9 proteins

Shahin Sultana[a], Md Ahad Hossain[a], Md Mazherul Islam[a] and Sarkar M. A. Kawsar[a*]

[a]Lab of Carbohydrate and Nucleoside Chemistry (LCNC), Department of Chemistry, Faculty of Science, University of Chittagong, Chittagong-4331, Bangladesh

CHRONICLE	ABSTRACT
	Methyl α-D-mannopyranoside (MAM) is a naturally occurring carbohydrate derivative that has gained attention in drug discovery due to its potential therapeutic applications, particularly as an antifungal agent. In this study, we employed a computational approach to investigate the interactions between MAM and two *Candida albicans* antifungal proteins, 1IYL and 1AI9, through molecular docking simulations. Furthermore, we performed a PASS (Prediction of Activity Spectra for Substances) analysis to predict MAM potential biological activities, explored the pharmacokinetic properties and ADMET (absorption, distribution, metabolism, excretion, and toxicity) profiles, and optimized the MAM using the density functional theory (DFT) method. The molecular docking results revealed favorable binding interactions between MAM and the active sites of the 1IYL and 1AI9 proteins, suggesting potential antifungal activity. Additionally, the ADMET profiles indicated low toxicity and suitable drug-like properties, such as moderate metabolic stability and minimal risk of adverse effects. Furthermore, DFT optimization was performed to investigate the molecular geometry and electronic properties of MAM. The optimization results provided valuable information on the stability and reactivity of MAM, enabling a better understanding of its chemical behavior and potential modifications for enhanced activity. Finally, PASS prediction was employed to evaluate MAM's potential biological activities beyond its antifungal properties. The analysis revealed several potential activities, including antibacterial, antiviral, and immunomodulatory effects, expanding the scope for future research and therapeutic applications. In conclusion, this computational study sheds light on the molecular interactions, pharmacokinetic properties, ADMET profiles, DFT optimization, and PASSES predictions of MAM. These findings highlight the potential of MAM as a promising antifungal agent with favorable pharmacological properties.

1. Introduction

Carbohydrates, the most abundant class of biomolecules on Earth, play pivotal roles in various biological processes. Composed of sugars, these macromolecules are involved in energy storage, cell signalling, immune response modulation, and structural integrity. Beyond their fundamental biological functions, carbohydrates have garnered significant attention for their medicinal value, with recent research unveiling their potential in drug discovery[1], immunotherapy, and disease treatment. Carbohydrates serve as the primary energy source for living organisms, fueling cellular processes and providing structural components for cells and tissues. Carbohydrates offer a significant portion of the energy that all organisms require for a variety of biological functions. Carbohydrates are essential for health and fitness since they are a key component of food and help to increase bodily strength by providing energy. They are one of three key macronutrients that provide significant energy; the other two macronutrients are fats and proteins. Sugars and starch operate as fuel for a quick energy supply, allowing one to accomplish physical tasks flawlessly. Carbohydrates enhance the flavor and look of a food item, making it more appealing and delectable. They also contribute to metabolism and intercell–cell interactions by providing the necessary energy[2,3]. Moreover, they play a critical role in cell recognition and signalling events, influencing intercellular

communication and immune responses. Glycosylation[4], the process of adding sugar moieties to proteins and lipids, impacts protein folding, stability, and cellular localization, further emphasizing the significance of carbohydrates in biological systems. Carbohydrates exhibit unique structural diversity and biological properties that make them valuable in medicinal applications. Glycans, a subset of carbohydrates, have been implicated in numerous diseases, including cancer, inflammation, and microbial infections. Exploiting the specific interactions between glycans and their associated proteins (lectins) has led to the development of carbohydrate-based vaccines, antiviral agents, and immunotherapies. Moreover, carbohydrates serve as important targets for drug discovery, providing opportunities for the development of therapeutics targeting carbohydrate-processing enzymes and carbohydrate-binding proteins. Another essential property of carbohydrate molecules is that they serve as an anti-agent for a variety of microbial species[5]. In a study of the literature, aromatic compounds (aromatic and heterocyclic) were shown to be enriched in biological capabilities[6-13]. In general, halogen, sulfur, and nitrogen-substituted aromatic compounds and their derivatives have a high potential for antibacterial efficiency enhancement[14-19]. Furthermore, regioselective acylation and antimicrobial activity screening of carbohydrate compounds revealed that the attachment of heterocyclic aromatic rings to electron-attracting or donating groups significantly improves the biological properties of the precursor molecules[20-22]. The addition of aliphatic and aromatic groups to the hydroxyl group of nucleoside and monosaccharide structures has resulted in the formation of effective antiviral[23-27] and antibacterial candidates[28,29]. Keeping these characteristics in mind, as well as the future goal of discovering novel drug agents[30-36] with biological importance[37-42], we reported the computational investigation of a number of methyl α-D-mannopyranoside-based analogs **2-7** with some rarely used aliphatic and aromatic groups, including molecular docking against bacterial and fungal proteins. Furthermore, the physicochemical and pharmacokinetic properties of all produced methyl α-D-mannopyranoside analogs were examined using density functional theory (DFT).

2. Results and Discussion

The modified derivatives of methyl α-D-mannopyranoside used in this study were previously synthesized, and the structures of the compounds are shown in **Fig. 1**.
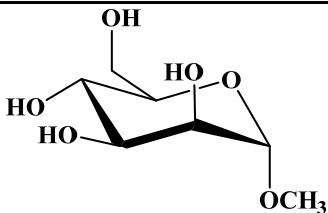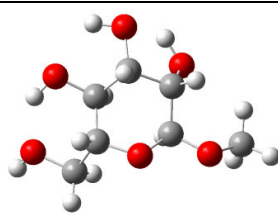
2.1 PASS prediction

Because significant adverse side effects and toxicity are unknown and only become apparent much too late, it appears that many research initiatives never make it to the final stage. However, using a simple internet server called PASS online, it is now feasible to predict more than 3678 pharmacological effects, modes of action, carcinogenicity, teratogenicity, and other biological features of substances. **Table 1** displays the PASS results in their designated Pa and Pi forms. The PASS predictions for the antibacterial, anti-carcinogenic, antifungal and anti-inflammatory properties of compounds **1–7** were determined to be 0.541, 0.731, 0.662 and 0.710, respectively. This showed that the chemicals were more effective against antifungal and cancer-causing substances.

Table 1. Data of pass prediction of methyl-α-D-mannopyranoside (**1**) and its derivatives (**2-7**).

| Entry	Antibacterial		Anti carcinogenic		Antifungal		Anti-inflammatory	
	Pa	Pi	Pa	Pi	Pa	Pi	Pa	Pi
1	0.541	0.013	0.731	0.008	0.628	0.016	0.650	0.023
2	0.521	0.015	0.635	0.011	0.629	0.016	0.626	0.027
3	0.540	0.013	0.496	0.020	0.662	0.012	0.612	0.029
4	0.472	0.036	0.314	0.053	0.542	0.024	0.710	0.014
5	0.540	0.013	0.496	0.020	0.662	0.012	0.612	0.029
6	0.540	0.013	0.496	0.020	0.662	0.012	0.612	0.029
7	0.483	0.025	0.449	0.007	0.498	0.034	0.548	0.044

Using the DFT approach under a 3-21G basis set for quantum computation and geometry optimization, the chemical properties of the generated ligands were further studied. **Table 2** mentions the geometrical structures of all produced compounds that have been optimized.

Table 2. Chemical and optimized structure of methyl-α-D-mannopyranoside (**1**) and its derivatives (**2–7**).
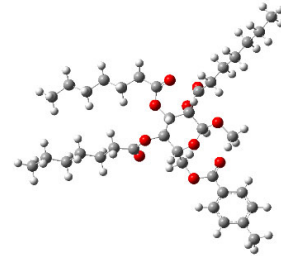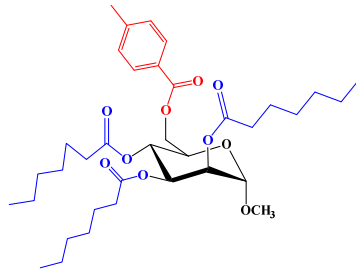
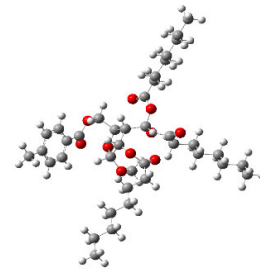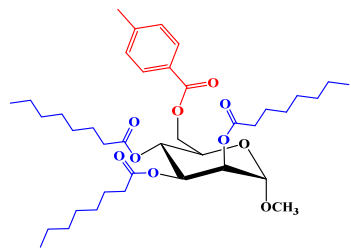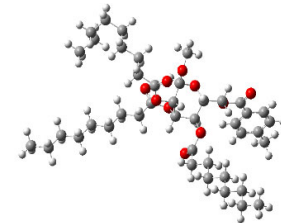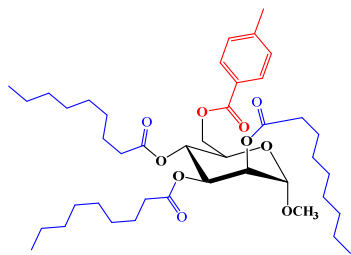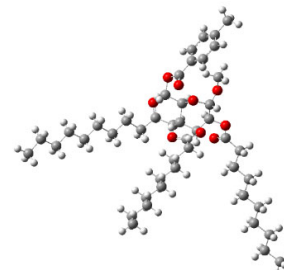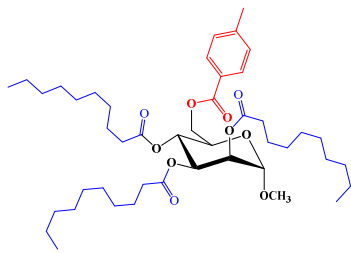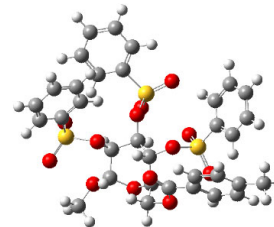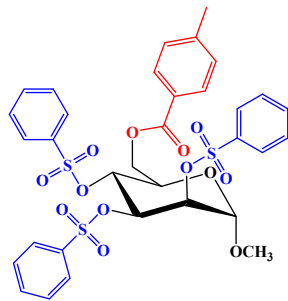| Entry	Structure	Optimized
1		
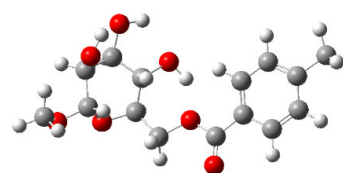
2
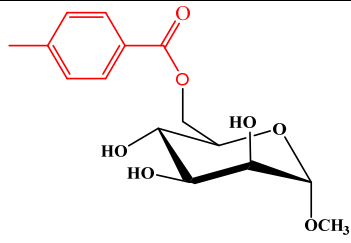
3

4

5

6

7

2.2 Thermodynamic analysis

Normal molecular structure changes have a large impact on structural characteristics, including thermal and molecular orbital parameters. The free energy and enthalpy values can be used to determine a reaction's spontaneity and the stability of a product[43].

Table 3. The stoichiometry, electronic energy, enthalpy, Gibbs free energy in Hartree, dipole moment (Debye) and polarizability (a.u.) of thymidine derivatives.

Entry	Stoichiometry	Electronic Energy (Hartree)	Enthalpy (Hartree)	Gibbs free Energy (Hartree)	Dipole moment (Debye)	Polarizability (a.u.)
1	$C_7H_{14}O_6$	-722.4610	-722.2228	-722.2765	4.5561	86.1880
2	$C_{15}H_{20}O_7$	-1104.0830	-1103.7161	-1103.7913	4.8377	168.2287
3	$C_{36}H_{56}O_{10}$	-2146.0920	-2145.1474	-2145.2982	5.3017	397.6397
4	$C_{39}H_{62}O_{10}$	-2263.3707	-2262.3361	-2262.4965	4.8676	415.4970
5	$C_{42}H_{68}O_{10}$	-2380.6881	-2379.5638	-2379.7325	5.4615	454.5317
6	$C_{46}H_{76}O_9$	-2462.2893	-2461.0490	-2461.2343	3.9850	494.1340
7	$C_{33}H_{32}O_{13}S_3$	-3430.4752	-3429.8125	-3429.9440	10.2680	407.9087

More negative values are indicative of enhanced thermal stability. Within drug design, the establishment of hydrogen bonds and nonbonded interactions is also influenced by the dipole moment. A higher dipole moment can also contribute to an improved binding property[44]. MAM (methyl-α-D-mannopyranoside) has a calculated free energy of -722.2765 Hartree, whereas the Gibbs free energy for compound **7** is -3429.9440 Hartree. Compound **7** exhibits the highest electronic energy (-3430.4752 Hartree) and the greatest dipole moment (10.2680 Debye). The incorporation of a bulky acylating group suggests a potential enhancement in polarizability; notably, compound **6** demonstrates the highest polarizability value (494.1340 a.u.). As the number of carbon atoms increased and the substituents incorporated aromatic rings with compounds **2** to **7**, all assessed variables exhibited increased assessments. Therefore, the thermodynamic properties of MAM compounds are significantly improved through the modification of their hydroxyl (-OH) groups[45].

2.3 Frontier molecular orbitals analysis

The most significant molecular orbitals of a molecule are known as the frontier orbitals, and they are thought to describe the chemical reactivity and kinetic stability of the molecule. The terms "highest occupied molecular orbital" (HOMO) and "lowest unoccupied molecular orbital" (LUMO) refer to these frontier molecular orbitals.

Table 4. Energy (eV) of HOMO, LUMO, energy gap, hardness and softness, chemical potential, electronegativity, and electrophilicity of analogs.

Entry	εHOMO	εLUMO	Gap	Hardness	Softness	chemical potential	electronegativity	electrophilicity
1	-6.3363	1.0711	7.4074	3.7037	0.2700	-2.6326	2.6326	0.9357
2	-6.4950	-1.5734	4.9216	2.4608	0.4064	-4.0342	4.0342	3.3068
3	-6.8378	-1.3154	5.5224	2.7612	0.3622	-4.0766	4.0766	3.0094
4	-6.5869	-0.9445	5.6424	2.8212	0.3545	-3.7657	3.7657	2.5132
5	-6.6158	-0.9358	5.6800	2.8400	0.3521	-3.7758	3.7758	2.5100
6	-6.5491	-1.0226	5.5265	2.7632	0.3619	-3.7859	3.7859	2.5935
7	-6.8139	-1.6618	5.1520	2.5760	0.3882	-4.2379	4.2379	3.4859

Table 4 presents the orbital energy values and includes two significant chemical descriptors: hardness and softness, which were computed for all compounds. Compound **2** exhibits the highest softness value among all compounds. On the other hand, compound **1** displays the greatest HOMO-LUMO gap and hardness values. These findings suggest that compound **1** possesses lower reactivity than the other compounds, aligning with the observations of Pearson et al[46]. The large energy difference of frontier molecular orbital molecules indicates strong chemical structural stability and weak reactivity. However, the outgoing of electrons from the stable level HOMO to the excited level LUMO demands additional energy[47].

In **Fig. 1**, the LUMO plot of compound 04 indicates electron localization on the upper portion of the MAM ring. Conversely, the HOMO plot reveals electron localization exclusively in the modified acylating group regions.
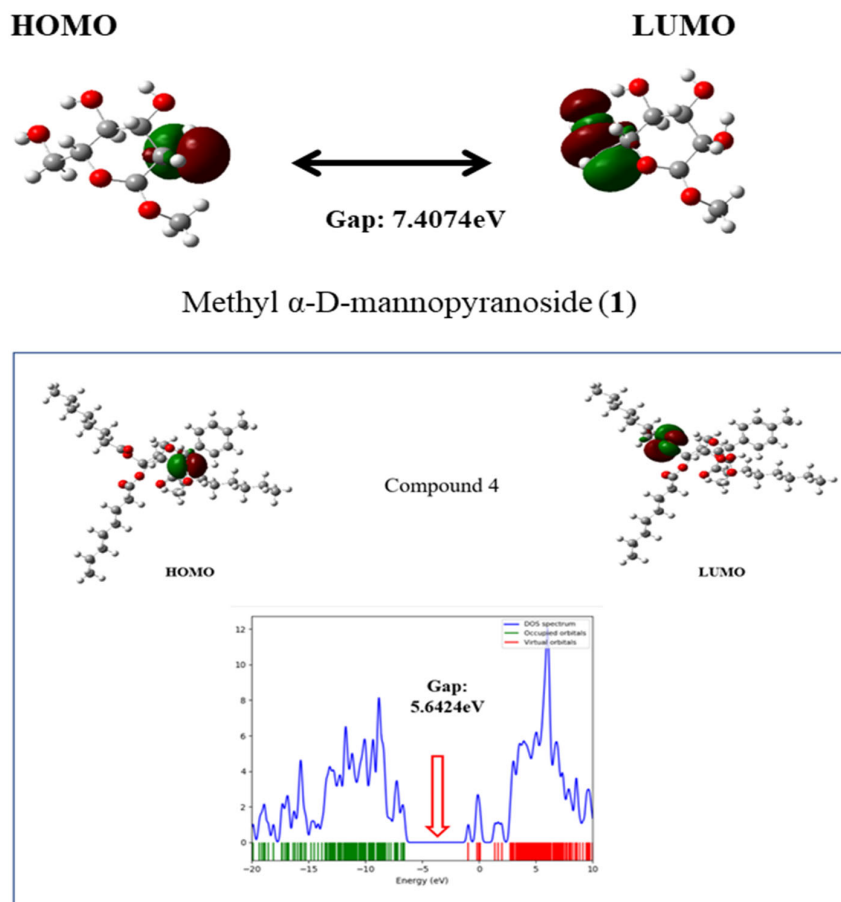
HOMO

LUMO

Gap: 7.4074eV

Methyl α-D-mannopyranoside (**1**)

Compound 4

HOMO

LUMO

Gap:
5.6424eV

Fig. 1. Molecular orbital distribution plots of HOMO &LUMO in the ground state of **01** and derivative **04** & DOS diagram

2.4 Molecular electrostatic potential (MEP)

As a reactivity map showing the most likely location for the electrophilic and nucleophilic attack of reagents with charged points on organic molecules[48], the molecular electrostatic potential (MEP) is frequently used. It aids in the interpretation of biological recognition mechanisms and hydrogen bonding relationships. To estimate how various geometries could interact, use the MEP counter map. The DFT model's basis set 3-21G optimization result was used to determine the MEP of MAM derivatives (**2** to **7**), which is shown in **Fig. 2**. The significance of MEP lies in the fact that it concurrently shows molecule size, shape, and positive, negative, and neutral electrostatic potential areas in terms of color grading and is extremely helpful in research on molecular structure with physicochemical attribute connections. The optimized structure of MAM derivatives (**2–7**) was used to compute the molecular electrostatic potential (MEP) and predict the reactive sites for electrophilic and nucleophilic attack. The different values of electrostatic potential are represented by different colors. Potential increases in the order red < orange < yellow < green < blue. Maximum electrophilic attack sites are shown in red, maximum nucleophilic attack sites are indicated in blue, and zero potential areas are indicated in green. Therefore, MEP may be useful to determine how complete charges (both positive and negative) are scattered over the surface of an individual molecule[49].
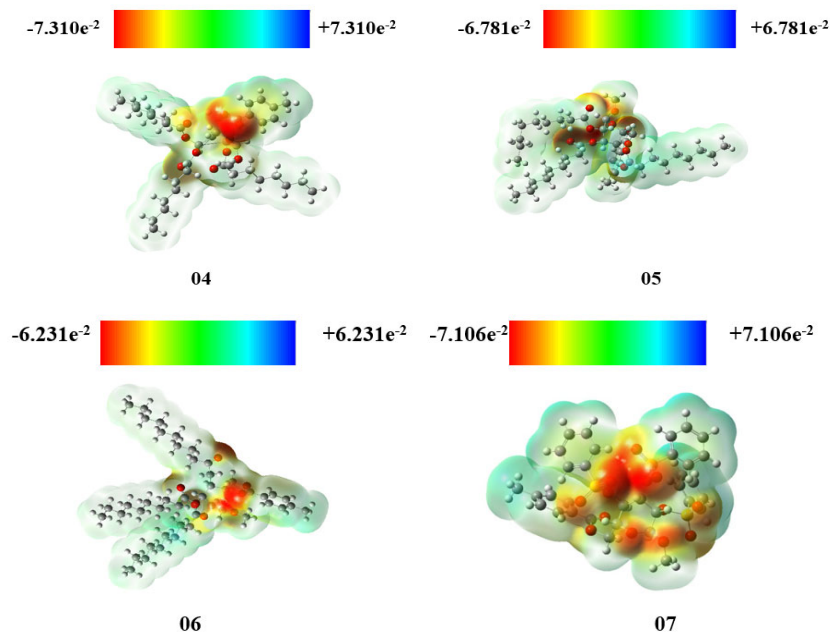
$-6.973e^{-2}$ $+6.973e^{-2}$ $-6.831e^{-2}$ $+6.831e^{-2}$

02   **03**
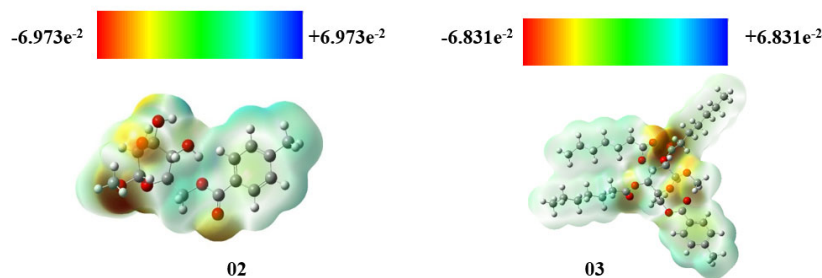
Fig. 2. Molecular electrostatic potential map of MAM derivatives

2.5 Pharmacokinetic prediction

To analyze whether the modified compounds produce any toxicity or altered pharmacokinetic profile, the admetSAR server was utilized. AdmetSAR is a web-based application for predicting ADME data and building a drug-like library using an in silico method. Different pharmacokinetic and pharmacodynamic parameters, such as human intestinal absorption[50] blood–brain barrier[51] P-glycoprotein inhibitor[52], cytochrome P450 inhibition[53], human ether-a-go-go-related gene inhibition[54], rat acute oral toxicity[55] and water solubility[56], were considered. The results are summarized in **Table 5**. As shown in **Table 5,** in the case of human intestinal absorption, if a compound with an HIA% is less than 30%, it is labeled HIA-; otherwise, it is labeled HIA+. All compounds revealed a positive value (value above the prescribed threshold, suggesting good permeability) with high probabilities. Furthermore, modifications of methyl α-D-mannopyranoside resulted in an inhibitor of P-glycoprotein. The analysis showed that methyl α-D-mannopyranoside derivatives were potential compounds of the human ether-a-go-go-related gene due to their lower value. The inhibitory feature of hERG can lead to long QT syndrome[57], which is why further investigation is required on this aspect. By the rules, all the compounds fell inside the permitted range. As a result, all of the substances had a favorable pharmacokinetic profile. The results also suggest that all derivatives tested may not inhibit the hERG channel and may not have oral toxicity. **Table 5** shows that MAM molecules are soluble[58].

Table 5. Selected pharmacokinetic parameters of methyl-α-D-mannopyranoside (**1**) and its derivatives (**2–7**).

Entry	Human Intestinal Absorption	Blood Brain Barrier	P-glycoprotein inhibitior	CYP2C19 inhibition	hERG	Acute Oral Toxicity	Water solubility
1	-0.9405	-0.6143	-0.9612	-0.9453	-0.5371	(III)0.4849	0.621
2	-0.8185	-0.5500	-0.8737	-0.9238	-0.7324	(III)0.7667	-1.16
3	+0.9591	-0.7286	+0.8482	+0.6248	+0.8478	(III)0.6375	-4.505
4	+0.9591	+0.7250	+0.8320	+0.6248	+0.7844	(III)0.6375	-4.505
5	+0.9591	+0.7250	+0.8186	+0.6248	+0.7848	(III)0.6375	-4.505
6	+0.9591	+0.7250	+0.7935	+0.6248	+0.7526	(III)0.6375	-4.505
7	+0.9228	+0.7250	+0.8866	-0.5819	+0.8662	(III)0.6069	-2.97

+ = Inhibitor, - = Non-Inhibitor, III = Category III includes compounds with LD50 greater than 500 mg/kg but less than 5000 mg/kg.

2.6 Molecular docking studies and ligand–protein interactions

Molecular docking is a technique that is frequently used in the field of molecular modeling to explore in-depth the interactions between a ligand and receptor and to establish the preferred orientation of this ligand to a target receptor. In fact, we employed two distinct receptors (PDB: 1IYL and 1AI9) to identify the optimal receptor for MAM ligands. These *C. albicans* crystal structures were taken from the Protein Data Bank. The three relevant receptors were prepared before starting the molecular docking computation by removing all water molecules and nonprotein components[59]. The analysis

revealed that MAM (**1**), which was found to be active in antibacterial and antifungal tests, exhibited binding affinities of -5.8 and -5.4 kcal mol^{-1} for both protease proteins, and the binding affinities of its derivatives (**2-7**) were approximately -7.7 to -9.0 kcal mol^{-1} for 1IYL and (-6.3 to -9.2) for 2Y7L (**Table 6**). We compared the current antifungal drugs fluconazole and voriconazole with our synthesized MAM analogs[60].

Table 6. Binding affinities (kcal/mol) of methyl-α-D-mannopyranoside (**1**) and its derivatives (**2–7**).

Entry	Main protease 1IYL				Main protease 1AI9			
	Binding Affinity	No. of Hydrogen Bond	No. of Hydrophobic Bond	Interaction type	Binding Affinity	No. of Hydrogen Bond	No. of Hydrophobic Bond	Interaction type
1	-5.8	3	-	H,C	-5.4	4	-	H,C
2	-7.8	3	4	H,C,PPT,A,PA	-7.3	4	5	H,PS,A,PA
3	-8.9	2	16	H,PS,PPS,PPT,A,PA	-6.6	3	4	H,C,A,PA
4	-7.7	4	17	H,C,PS,PPT A,PA	-6.5	2	9	H,PS,A,PA
5	-7.6	4	13	H,C,PS,PPT A,PA	-6.7	3	16	H,C,PS,PPS,A,PA
6	-7.7	3	15	H,C,PS,A,PA	-6.3	9	12	H,C,PPT,A,PA
7	-9.0	4	9	H,C,PS,PPTPPS,PA	-9.2	2	7	H,C,PPS,PA
Fluconazole	-8.0	5	6	H,C,PPT,PPS,PA	-6.8	5	7	H,C, PPS,PA,
Voriconazole	-8.3	5	8	H,C,PPT,PPS,PA	-6.7	3	4	H,C,PPS,PA

H = Conventional hydrogen bond; C = Carbon–hydrogen bond; A= alkyl; PA = Pi–alkyl; PPS = Pi–Pi stacked; PS = Pi–Sigma; PPT = Pi–Pi T-shaped.

Table 7. Nonbonding interactions of derivatives with amino acid residues of MAM and **07** with antifungal drugs.

	Main protease 1IYL					Main protease 1AI9			
	Hydrogen Bond		Hydrophobic Bond			Hydrogen Bond		Hydrophobic Bond	
Drug	Residues	Distance (Å)	Residues	Distance (Å)	Drug	Residues	Distance (Å)	Residues	Distance (Å)
1	HIS307	2.32548	--	--	**1**	ARG191	2.52284		
	ASP312	2.09993				SER125	2.11637		
	GLU122	3.44301				SER125	3.50945		
7	THR211	2.03791	LEU415	3.9168		LYS192	3.54142		
	ASP110	3.27159	PHE117	4.9591	**7**	SER61	2.09414	PHE36	4.37241
	GLY213	2.73953	LEU394	5.31756		GLY23	3.26125	ILE62	5.18124
	TYR225	3.2618	PHE117	5.43932				ALA115	4.33478
			TYR225	5.52508				ALA11	4.97573
			TYR225	4.72146				MET25	5.24074
			PHE339	5.1106				LEU69	5.36484
			ILE111	5.18285					
FLUCONAZOLE	TYR225	2.12385	PHE240	3.88488	FLUCONAZOLE	VAL109	2.87129	ASN5	3.15215
	ASN392	2.89777	PHE115	5.05747		SER94	2.66122	GLU107	3.1627
	TYR225	2.87925	PHE339	5.28604		GLU107	2.2037	PRO4	5.12577
	HIS227	3.32347	PHE117	5.40353		ARG108	3.16427	MET1	4.83122
			TYR225	4.90773				HIS129	5.41631
			ILE352	5.28747					
VORICONAZOLE	THR211	2.83984	PHE117	5.25971	VORICONAZOLE	SER94	2.65466	ASN83	3.04852
	THR211	3.36817	TYR225	4.85474				SER94	3.61266
	TYR335	3.58239	LEU415	5.31736				GLU82	4.0865
			LEU337	5.4105				ARG108	4.48375
			LEU415	5.34936				MET1	4.63082
			LEU394	4.87502					

In the context of this research, we explored the interaction profiles of antifungal drugs, specifically fluconazole and voriconazole, within the active sites of two main protease enzymes, 1IYL and 1AI9[61,62]. These interactions encompass both hydrogen bonding and hydrophobic contacts, which are pivotal in understanding the mechanisms of drug binding. Notably, the examined compounds display varying interaction patterns. Compound **7**, with its distinctive *p*-toluoyl and benzene sulfonyl groups, which are substituted by primary and secondary hydroxyl groups, provides a high gathering of electrons in the molecule, indicating the highest binding score, and engages in hydrogen bonds with key residues within the enzymes while also forming hydrophobic bonds. Noteworthy interactions involve specific residues such as HIS307, ASP312, and GLU122 for compound **1** in enzyme 1IYL and ARG191 and SER125 for compound **1** in enzyme 1AI9. Similarly, compound **7** exhibits interactions with residues such as THR211, ASP110, GLY213, and TYR225 in enzyme 1IYL and SER61, PHE36, ILE62, and ALA115 in enzyme 1AI9. These interactions, along with the unique structural modifications of compound **7**, suggest potential avenues for enhancing binding affinity. Additionally, fluconazole and voriconazole, known antifungal agents, exhibit intricate networks of interactions involving aromatic residues, hydrophobic interactions, and hydrogen bonds, which are crucial for understanding their mode of action. Further research into these interactions could offer valuable insights into optimizing the design of antifungal drugs for improved efficacy. Due to hydrogen bonding, some

compounds have higher binding energies and modes. The modifications of the -OH group in MAM strengthened the π-π interactions with the amino acid chain at the binding site, while their polarity improvement caused hydrogen bond interactions[63].

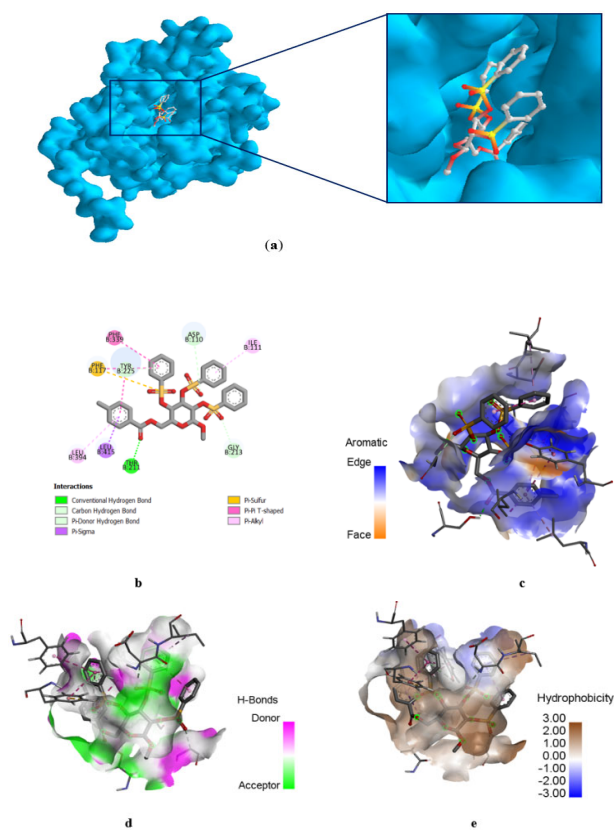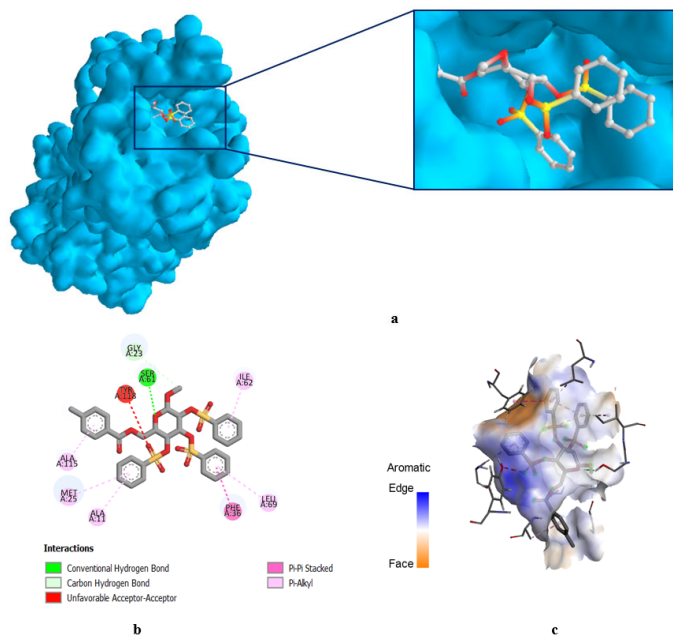**Fig. 3.** (**a**) Docked pose of compound **7** with 1IYL; (**b**) nonbonding interactions of compound (**7**) with the active site of 1IYL; (**c**) aromaticity; (**d**) hydrogen bonds; and (**e**) hydrophobicity were determined by Discovery Studio.
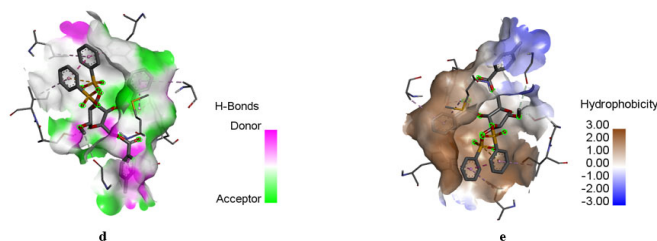
Fig. 4. (a) Docked pose of compound **7** with **1AI9**. **(b)** Nonbonding interactions of compound (**7**) with the active site of 1AI9. **(c)** Aromaticity. **(d)** Hydrogen bonds. **(e)** Hydrophobicity was determined by Discovery Studio.

3. Conclusions

In conclusion, the optimization of compound structures through DFT calculations provided stable conformations, facilitating further analysis of their properties and interactions. The calculation of thermodynamic properties offered insights into the stability, reactivity, and potential binding interactions of the compounds. The PASS prediction analysis predicted the potential biological activities of the compounds, highlighting their potential as antifungal agents against *Candida albicans.* This information guided the selection of compounds for further investigation. Evaluation of ADMET properties provided valuable information on the compounds' drug-like characteristics and safety profiles. Favorable ADMET properties indicated their potential for further development as drug candidates with optimal pharmacokinetic and toxicological profiles. Molecular docking analysis with *Candida albicans* proteins 1IYL and 1AI9 elucidated the binding modes and interactions between the optimized compounds and the target proteins[56]. The analysis revealed the formation of hydrogen bonds, hydrophobic contacts, and other molecular interactions, providing insights into the compounds' potential inhibitory effects. The integrated approach employed in this study contributes to a comprehensive understanding of the potential antifungal activity of novel compounds against *Candida albicans*. The results lay the foundation for future experimental investigations and optimization of the identified compounds as potential inhibitors, ultimately aiming to develop effective antifungal therapeutics. Overall, this journal article presents valuable findings and methodologies that contribute to the field of antifungal drug discovery and provides a platform for further research and development in the fight against *Candida albicans* infections.

Acknowledgments

Conflict of interest

The authors declare no conflicts of interest.

4. Experimental

4.1. Software used

These software applications were used during the current analysis: Gaussian 09, Gaussum 3.0, PyRx 0.8, Swiss-Pdb 4.1.0, Discovery Studio 3.5, PyMOL 2.3, Hyperchem-8.0.1, and ChemDraw-21.0.

4.2. Structural optimization

In this experiment, a variety of chemicals were examined using the Gaussian 09 program[64]. The drawing of the structures was performed using GaussView 6. The molecular structure must first be optimized using DFT (density functional theory) and the B3LYP technique with a basis set of 3-21G to predict and optimize the thermal and molecular orbital properties of the compounds. This is the first step in obtaining the leading characteristic parameters of the compounds. Calculations were made for each analog's dipole moment, enthalpy, free energy, and electrical energy. These structures were used for molecular docking, molecular reactivity descriptors, ADMET, and QSAR calculations once they had been optimized.

4.3. Computation of descriptors for chemical reactivity

The values of chemical reactivity and related descriptors were obtained using a variety of calculation techniques in acceptable formats[65,66]. At the same level of theory, the frontier molecular orbital properties HOMO (highest occupied molecular orbital) and LUMO (lowest unoccupied molecular orbital) were counted. Given the reported energies of the frontier HOMO and LUMO and taking into account Parr and Pearson's interpretation of DFT as well as Koopman's

theorem[67] on the correlation of chemical potential (μ), electronegativity (χ), and electrophilicity (ω) with HOMO and LUMO energy (ε), the HOMO-LUMO energy gap, hardness (η), and softness (S) were calculated for each of the methyl alpha-D-mannopyranoside analogs. By examining molecular orbital characteristics, the following equations were utilized to determine the overall chemical reactivity.

$$\text{HOMO-LUMO energy gap } (\Delta\varepsilon) = \varepsilon\text{LUMO} - \varepsilon\text{HOMO}$$

$$\text{Hardness } (\eta) = \frac{[\varepsilon\text{LUMO} - \varepsilon\text{HOMO}]}{2}$$

$$\text{chemical potential } (\mu) = \frac{[\varepsilon\text{LUMO} + \varepsilon\text{HOMO}]}{2}$$

$$\text{electronegativity } (\chi) = -\frac{[\varepsilon\text{LUMO} + \varepsilon\text{HOMO}]}{2}$$

$$\text{electrophilicity } (\omega) = \frac{\mu2}{2\eta}$$

$$\text{and softness (S)} = \frac{1}{2\eta}$$

4.4. PASS predictionα

Using web-based PASS (prediction of activity spectra for pharmaceuticals; http://www.pharmaexpert.ru/PASSonline/index.php), a broad variety of biological processes were predicted. With 90% accuracy[68], this technique was created to forecast a wide range of biological activities. ChemDraw 21.0 was used to generate the structures, which were then saved in Smiles format and utilized with the PASS online version to predict the biological spectrum. The outcome was represented by the probabilities Pa (for the active compound) and Pi (for the inactive molecule). On a scale of 0.000 to 1.000, Pa > Pi is considered in this situation, and frequently, Pa + Pi 1. The PASS prediction results were used and interpreted in various ways, including [i] when Pa > 0.7, the chance to find the activity experimentally is high; [ii] if 0.5 Pa 0.7, the chance to find the activity experimentally is less, but the compound is probably not as similar to known pharmaceutical agents; and [iii] if Pa 0.5, the chance to find the activity experimentally is less but not the chance to find structurally[69]. As a result, the compound's intrinsic property is defined as the predicted activity of the spectrum.

4.5. Preparation and visualization of proteins

These proteins, which were retrieved from the protein data library at http://www.ecsb.org, identify many C. albicans proteins in their crystal 3D structures. Using the PYMOL tool (Version: 2.5.3), the water molecules and other ligands that had been attached to the protein before were removed to create the raw protein strain for molecular docking. After that, Swiss-Pdb Viewer (version 4.1.0) was used to subject the proteins to energy reduction.

4.6. Studies on molecular docking

In PyRx, ligands and proteins (macromolecules) were opened. The ligands were changed to PDBQT format once the energy was reduced. Vina wizard was assigned to dock the protein and its ligands with the largest possible box size. The produced file was saved for later analysis using the BIOVIA Discovery Studio Visualizer.

4.7. ADMET and drug likeness parameter prediction

Computer simulation is employed in computational chemistry to aid in the resolution of chemical issues. It utilizes effective computer algorithms and theoretical chemistry techniques to calculate the physical and chemical properties of the synthesized molecules. For systems in the solid, gas, or solution phase, molecular energies and structures, transition state structures, bond and reaction energies, molecular orbitals in various solvent phases, vibrational frequencies, thermochemical properties, reaction pathways, spectroscopic quantities, and many other molecular properties can be predicted. Using their chemical structures, drug-like substances can have their pharmacokinetic properties and features estimated using an online server called admetSAR[70]. AdmetSAR predicts the physicochemical characteristics, absorption, distribution, metabolism, elimination, and pharmacokinetic features of molecules—all of which are crucial elements for upcoming clinical trials. This study may be used to lay the groundwork for a laboratory synthesis and to aid in comprehending the findings of experiments.

References

1.   Nogueira C. M., Parmanhan B. R., Farias P. P., Corrêa A. G. (**2009**) An Importância Crescente Dos Carboidratos Em Química Medicinal. *Rev. Virt. Quím.*, 1 149–159.

2.   Sears P., Wong C. H. (**1996**) Intervention of Carbohydrate Recognition by Proteins and Nucleic Acids. *Proc. Natl. Acad. Sci. USA*, 93 12086–12093.

3.   Seeberger P. H., Werz D. B. (**2007**) Synthesis and medical applications of oligosaccharides. *Nature*, 446 1046–1051.

4.   Varki A. et al. (Eds.) (**2015**) Essentials of Glycobiology. Cold Spring Harbor Laboratory Press.

5.   Chen S., Fukuda M. (**2006**) Cell type-specific roles of carbohydrates in tumor metastasis. *Meth. Enzymol.*, 416 371–380.

6.   Kawsar S. M. A., Islam M., Jesmin S., Manchur M. A., Hasan I., Rajia S. (**2018**) Evaluation of the antimicrobial activity and cytotoxic effect of some uridine derivatives. *Int. J. Biosci.*, 12 211–219.

7.   Kawsar S. M. A., Hamida A. A., Sheikh A. U., Hossain M. K., Shagir A. C., Sanaullah A. F. M., Manchur M. A., Imtiaj H., Ogawa Y., Fujii Y., et al. (**2015**) Chemically modified uridine molecules incorporating acyl residues to enhance antibacterial and cytotoxic activities. *Int. J. Org. Chem.*, 5 232–245.

8.   Shagir A. C., Bhuiyan M. M. R., Ozeki Y., Kawsar S. M. A. (**2016**) Simple and rapid synthesis of some nucleoside derivatives: Structural and spectral characterization. *Curr. Chem. Lett.*, 5 83–92.

9.   Rana K. M., Ferdous J., Hosen A., Kawsar S. M. A. (**2020**) Ribose moieties acylation and characterization of some cytidine analogs. *J. Sib. Fed. Univ. Chem.*, 13 465–478.

10. Bulbul M. Z. H., Chowdhury T. S., Misbah M. M. H., Ferdous J., Dey S., Hasan I., Fujii Y., Ozeki Y., Kawsar S. M. A. (**2021**) Synthesis of new series of pyrimidine nucleoside derivatives bearing the acyl moieties as potential antimicrobial agents. *Pharmacia*, 68 23–34.

11. Arifuzzaman M., Islam M. M., Rahman M. M., Mohammad A. R., Kawsar S. M. A. (**2018**) An efficient approach to the synthesis of thymidine derivatives containing various acyl groups: Characterization and antibacterial activities. *ACTA Pharm. Sci.*, 56 7–22.

12. Maowa J., Alam A., Rana K. M., Hosen A., Dey S., Hasan I., Fujii Y., Ozeki Y., Kawsar S. M. A. (**2021**) Synthesis, characterization, synergistic antimicrobial properties and molecular docking of sugar modified uridine derivatives. *Ovidius. Univ. Ann. Chem.*, 32 6–21.

13. Alam A., Hosen M. A., Hosen A., Fujii Y., Ozeki Y., Kawsar S. M. A. (**2021**) Synthesis, characterization, and molecular docking against a receptor protein FimH of Escherichia coli (4XO8) of thymidine derivatives. *J. Mex. Chem. Soc.*, 65 256–276.

14. Rana K. M., Maowa J., Alam A., Hosen A., Dey S., Hasan I., Fujii Y., Ozeki Y., Kawsar S. M. A. .(**2021**) In silico DFT study, molecular docking, and ADMET predictions of cytidine analogs with antimicrobial and anticancer properties. In Silico *Pharmacol.*, 9 42.

15. Farhana Y., Amin M. R., Hosen A., Kawsar S. M. A. (**2021**) Bromobenzoylation of methyl α-D-mannopyranoside: Synthesis and spectral characterization. *J. Sib. Fed. Univ. Chem.*, 14 171–183.

16. Devi S. R., Jesmin S., Rahman M., Manchur M. A., Fujii Y., Kanaly R. A., Ozeki Y., Kawsar S. M. A. (**2019**) Microbial efficacy and two-step synthesis of uridine derivatives with spectral characterization. *ACTA Pharm. Sci.*, 57 47–68.

17. Alam A., Hosen M. A., Islam M., Ferdous J., Fujii Y., Ozeki Y., Kawsar S. M. A. (**2021**) Synthesis, Antibacterial and cytotoxicity assessment of modified uridine molecules. *Curr. Adv. Chem. Biochem.*, 6 114–129.

18. Kawsar S. M. A., Kumar A. (**2021**) Computational investigation of methyl α-D-glucopyranoside derivatives as inhibitor against bacteria, fungi and COVID-19 (SARS-2). *J. Chill. Chem. Soc.*, 66 5206–5214.

19. Mirajul M. I., Arifuzzaman M., Monjur M. R., Rahman A., Kawsar S. M. A. (**2019**) Novel methyl 4,6-O-benzylidene-α-D-glucopyranoside derivatives: Synthesis, structural characterization and evaluation of antibacterial activities. *Hacet. J. Biol. Chem.*, 47 153–164.

20. Kawsar S. M. A., Faruk M. O., Rahman M. S., Fujii Y., Ozeki Y. (**2014**) Regioselective synthesis, characterization and antimicrobial activities of some new monosaccharide derivatives. *Sci. Pharm.*, 82 (1) 1–20.

21. Kawsar S. M. A., Hasan T., Chowdhury S. A., Islam M. M., Hossain M. K., Mansur M. A. (**2013**) Synthesis, spectroscopic characterization and in vitro antibacterial screening of some D-glucose derivatives. *Int. J. Pure App Chem.*, 8 125–135.

22. Misbah M. M. H., Ferdous J., Bulbul M. Z. H., Chowdhury T. S., Dey S., Hasan I., Kawsar S. M. A. (**2020**) Evaluation of MIC, MBC, MFC and anticancer activities of acylated methyl β-D-galactopyranoside esters. *Int. J. Biosci.*, 16 299–309.

23. Maowa J., Hosen M. A., Alam A., Rana K. M., Fujii Y., Ozeki Y., Kawsar S. M. A. (**2021**) Pharmacokinetics and molecular docking studies of uridine derivatives as SARS-CoV-2 Mpro inhibitors. *Phys. Chem. Res.*, 9 385–312.

24. Hosen M. A., Alam A., Islam M., Fujii Y., Ozeki Y., Kawsar S. M. A. (**2021**) Geometrical optimization, PASS prediction, molecular docking, and in silico ADMET studies of thymidine derivatives against FimH adhesin of *Escherichia coli*. *Bulg. Chem. Commun.*, 53 327–342.

25. Kawsar S. M. A., Kumer A., Munia N. S., Hosen M. A., Chakma U., Akash S. (**2022**) Chemical descriptors, PASS, molecular docking, molecular dynamics and ADMET predictions of glucopyranoside derivatives as inhibitors to bacteria and fungi growth. *Org. Commun.*, 15 1-20.

26. Farhana Y., Amin M. R., Hosen M. A., Bulbul M. Z. H., Dey S., Kawsar S. M. A. (**2021**) Monosaccharide derivatives: Synthesis, antimicrobial, PASS, antiviral, and molecular docking studies against SARS-CoV-2 m^pro inhibitors. *J. Cellul. Chem. Technol.*, 55 477–499.

12

27. Kawsar S. M. A., Bulbul M. Z. H., Hosen M. A., Ferdous J., Misbah M. M. H., Chowdhury T. S. (**2021**) Thermochemical, DFT study, physicochemical, molecular docking and ADMET predictions of some modified uridine derivatives. *Int. J. New Chem*., 8 88–110.

28. Kawsar S. M. A., Hosen M. A., Chowdhury T. S., Rana K. M., Fujii Y., Ozeki Y. (**2021**) Thermochemical, PASS, Molecular Docking, Drug-Likeness and In Silico ADMET Prediction of Cytidine Derivatives Against HIV-1 Reverse Transcriptase. *Rev. de Chim*., 72 159–178.

29. Kawsar S. M. A., Hosen M. A. (**2020**) An optimization and pharmacokinetic studies of some thymidine derivatives. *Turk. Comp. Theo. Chem*., 4 59–66.

30. Kawsar S. M. A., Almalki F. A., Hadd T. B., Hamid L., Khan M. A. R., Hosen M. A., Shafi M., Abdelouahed A., Maideen N. M. P., Fariba H., et al. (**2022**) Potential antifungal activity of novel carbohydrate derivatives validated by POM, molecular docking and molecular dynamic simulations analyses. *Mol. Simul.*, 48 1–16.

31. Amin M. R., Yasmin F., Hosen M. A., Dey S., Mahmud S., Saleh M. A., Hasan I., Fujii Y., Yamada M., Ozeki Y., et al. (**2021**) Synthesis, antimicrobial, anticancer, PASS, molecular docking, molecular dynamic simulations and pharmacokinetic predictions of some methyl β-D-galactopyranoside analogs. *Molecules*, 26 1–25.

32. Amin M. R., Yasmin F., Dey S., Mahmud S., Saleh M. A., Emran T. B., Hasan I., Rajia S., Ogawa Y., Fujii Y., et al. (**2021**) Methyl β-D-galactopyranoside esters as potential inhibitors for SARS-CoV-2 protease enzyme: Synthesis, antimicrobial, PASS, molecular docking, molecular dynamics simulations and quantum computations. *Glycoconj. J.*, 39 261-290.

33. Alam A., Rana K. M., Hosen M. A., Dey S., Bezbaruah B., Kawsar S. M. A. (**2022**) Modified thymidine derivatives as potential inhibitors of SARS-CoV: PASS, in vitro antimicrobial, physicochemical and molecular docking studies. *Phys. Chem. Res.*, 10 391–409.

34. Islam S., Hosen M. A., Ahmad S., Qamar M. T., Dey S., Hasan I., Fujii Y., Ozeki Y., Kawsar S. M. A. (**2022**) Synthesis, antimicrobial, anticancer activities, PASS prediction, molecular docking, molecular dynamics and pharmacokinetic studies of designed methyl α-D-glucopyranoside esters. *J. Mol. Struct*., 1260C 132761.

35. Kawsar S. M. A., Hosen M. A., El Bakri Y., Ahmad S., Sopi T. A., Goumri-Said S. (**2022**) In silico approach for potential antimicrobial agents through antiviral, molecular docking, molecular dynamics, pharmacokinetic and bioactivity predictions of galactopyranoside derivatives. *Arab J. Basic Appl. Sci*., 29 99–112.

36. Kawsar S. M. A., Ouassaf M., Hosen M. A., Chtita S., Qais F. A., Belaidi S. (**2022**) Physicochemical, ADMET, molecular docking and molecular dynamics simulations against Bacillus subtilis HmoB for antibacterial potentiality of methyl α-D-glucopyranoside derivatives. *Philipp. J. Sci*., 151 1393–1417.

37. Kawsar S. M. A., Hosen M. A., Fujii Y., et al. (**2020**) Thermochemical, DFT, molecular docking and pharmacokinetic studies of methyl β-D-galactopyranoside esters. *J. Comput. Chem. Mol. Model.,* 4 452–462.

38. Kawsar S. M. A., Matsumoto R., Fujii Y., et al. (**2011**) Cytotoxicity and glycan-binding profile of α-D-galactose-binding lectin from the eggs of a Japanese sea hare (*Aplysia kurodai*). *The Protein J.,* 30 509–519.

39. Kabir A. K. M. S., Kawsar S. M. A., Bhuiyan M. M. R., et al. (**2009**) Antimicrobial screening of some derivatives of methyl α-D-glucopyranoside. *Pak. J. Sci. Ind. Res*., 52 138–142.

40. Kabir A. K. M. S., Kawsar S. M. A.,Bhuiyan M. M. R., et al. (**2004**) Biological evaluation of some mannopyranoside derivatives. *Bull. Pure Appl. Sci*., 23 83–91.

41. Kabir A. K. M. S., Kawsar S. M. A.,Bhuiyan M. M. R., et al. (**2008**) Biological evaluation of some octanoyl derivatives of methyl 4,6-*O*-cyclohexylidene-α-D-glucopyranoside. *Chittagong Univ. J. Biol. Sci.,* 3 53–64.

42. Fujii Y., Kawsar S. M. A., Matsumoto R., et al. (**2011**) A-D-galactose-binding lectin purified from coronate moon turban, *Turbo (Lunella) coreensis*, with a unique amino acid sequence and the ability to recognize lacto-series glycophingolipids. *Comp. Biochem. Physiol.,* 158B 30–37.

43. Sim F., St-Amant A., Papai I., Salahub D. R. (**1992**) Gaussian Density Functional Calculations on Hydrogen-Bonded systems. *J. Am. Chem. Soc*., 114(11), 4391–4400.

44. Heinz H., Suter U. W. (**2004**) Atomic Charges for Classical Simulations of Polar Systems. *J. Phys. Chem*., 108, 18341–18352.

45. Cohen N., Benson S. W. (**1993**) Estimation of heats of formation of organic compounds by additivity methods. *Chem. Rev.,* 93 2419–2438.

46. Pearson R. G. (**1986**) Absolute electronegativity and hardness correlated with molecular orbital theory. *Proc. Natl. Acad Sci*., 83, 8440-8441

47. Saravanan S., Balachandran V. (**2014**) Quantum chemical studies, natural bond orbital analysis and thermodynamic function of 2,5-di-chlorophenylisocyanate. *Spectrochimica Acta Part A: Mol. Biomol. Spectrosc*., 120 351–364.

48. Hosen M. A., Munia N. S., Al-Ghorbani M., Baashen M., Almalki F. A., Hadda T. B., Ali F., Mahmud S., Saleh M. A., Laaroussi H., Kawsar S. M. A. (**2022**) Synthesis, antimicrobial, molecular docking, and molecular dynamics studies of lauroyl thymidine analogs against SARS-CoV-2: POM study and identification of the pharmacophore sites. *Bioorg. Chem.*, 125, 105850.

49. Politzer P., Murray J. S. (**1991**) Molecular electrostatic potentials and chemical reactivity. *Rev. Comput. Chem*., 2 273–312.

50. Shen J., Cheng F., Xu Y., Li W., Tang Y. (**2010**) Estimation of ADME Properties with Substructure Pattern Recognition. *J. Chem. Inf. Model*., 50 (6) 1034-1041

51. Wang Z., Yang H., Wu Z., et al. (**2018**) In Silico Prediction of Blood–Brain Barrier Permeability of Compounds by Machine Learning and Resampling Methods. *Chem. Med. Chem*., 13 (20) 2189-2201.

52. Chen L., Li Y., Zhao Q., Peng H., Hou T. (**2011**) ADME Evaluation in Drug Discovery. 10. Predictions of P-Glycoprotein Inhibitors Using Recursive Partitioning and Naive Bayesian Classification Techniques. *Mol. Pharm*., 8 (3) 889-900.

53. Cheng F., Yu Y., Shen J., et al. (**2011**) Classification of Cytochrome P450 Inhibitors and Noninhibitors Using Combined Classifiers. *J. Chem. Inf. Model*., 51 (5) 996-1011.

54. Sun L., Zhang C., Chen Y., et al. (**2015**) In silico prediction of chemical aquatic toxicity with chemical category approaches and substructural alerts. *Toxicol Res (Camb)*., 4 (2) 452-463.

55. Zhu H., Martin TM, Ye L., Sedykh A., Young DM, Tropsha A. (**2009**) Quantitative Structure−Activity Relationship Modeling of Rat Acute Toxicity by Oral Exposure. *Chem Res Toxicol*., 22 (12) 1913-1921.

56. Wang J., Krudy G., Hou T., Zhang W., Holland G., Xu X. (**2007**) Development of Reliable Aqueous Solubility Models and Their Application in Druglike Analysis. *J. Chem. Inf. Model*., 47 (4) 1395-1404.

57. Huang F.D., Chen J, Lin M, Keating MT, Sanguinetti MC. (**2001**) Long-QT Syndrome-Associated Missense Mutations in the Pore Helix of the HERG Potassium Channel. *Circulation*., 104 (9) 1071-1075.

58. Hirata K., Uchida T., Nakajima Y., Maekawa T., Mizuki T. (**2008**) Chemical Synthesis and Cytotoxicity of Neo-Glycolipids; Rare Sugar-Glycerol-Lipid Compounds**.** *Heliyon*, 4, e00861.

59. Zawadzińska K. & Gostyński B. (**2023**) Nitrosubstituted analogs of isoxazolines and isoxazolidines: a surprising estimation of their biological activity via molecular docking. *Sci. Rad.,* 2 25–46.

60. Mandloi D., Dabade S. J., Bajaj A. V & Atre H. (**2020**) Molecular Docking and QSAR studies for Modeling Antifungal Activity of Triazine Analogs against Therapeutic Target NMT of Candida albicans. *Int. J. Pharm. Sci. Drug Res*., 13 140–146.

61. Kawsar S. M. A. (**2023**) Galactopyranoside Derivatives as Potential Antibacterial Therapeutic Drugs for Pharmaceutical Uses. in *Novel Aspect. Chem. Biochem.*, 6 167–192.

62. Ahmmed F., Islam A., Mukhrish Y., et al. (**2022**) Efficient Antibacterial/Antifungal Activities: Synthesis, Molecular Docking, Molecular Dynamics, Pharmacokinetic, and Binding Free Energy of Galactopyranoside Derivatives. *Molecules* 28 219.

63. Liu X., Wang X. J. (**2020**) Potential inhibitors against 2019-nCoV coronavirus M protease from clinically approved medicines. *J. Genet. Genom*., 7 119–121.

64. Frisch M. J., Trucks G. W., Schlegel H. B., Scuseria G. E., Robb A., Cheeseman J. R., Scalmani G., Barone V., Mennucci B., Petersson G. A., et al. (**2009**) Gaussian 09. Gaussian Inc, Wallingford, CT.

65. Becke A. D. (**1988**) Density-functional exchange-energy approximation with correct asymptotic behavior. *Physical Review A*, 38 (6) 3098-3100.

66. Lee C., Yang W., Parr R. G. (**1988**) Development of the colle-Salvetti correlation-energy formula into a functional of the electron density. *Physical Review B*, 37 (2) 785-789.

67. Koopmans T. (**1934**) Über die Zuordnung von Wellenfunktionen und Eigenwerten zu den Einzelnen Elektronen Eines Atoms. *Physica*., 1 (1) 104-113.

68. Kumaresan S., Senthilkumar V., Stephen A., Balakumar B. S. (**2015**) GC–MS Analysis and PASS-Assisted Prediction of Biological Activity Spectra of Extract of Phomopsis sp. solated From Andrographis paniculata. *World J. Pharm. Res*., 4 1035–1053.

69. Filimonov D. A., Lagunin A. A., Gloriozova T. A., Rudik A. V. et al (**2014**) Prediction of the biological activity spectra of organic compounds using the PASS online web resource. *Chem. Heter. Comp. Russian Orig.*, 50 (3) 444–457.

70. Yang H., Lou C., Sun L., Li J., Cai Y. (**2019**) AdmetSAR 2.0: Web-service for prediction and optimization of chemical ADMET properties. *Bioinformatics*, 35 (6) 1067–1069.